MIMO RADAR PERFORMANCE ANALYSIS UNDER K-DISTRIBUTED CLUTTER

Xin Zhang, Mohammed Nabil El Korso, Marius Pesavento

MIMO RADAR PERFORMANCE ANALYSIS UNDER K-DISTRIBUTED CLUTTER

Xin Zhang**, Mohammed Nabil El Korso*** *and Marius Pesavento**

*Communication Systems Group, Technische Universität Darmstadt, Darmstadt, Germany
**Laboratoire Energétique Mécanique Electromagnétisme,
Université Paris Ouest Nanterre La Défense, Ville d'Avray, France

ABSTRACT

The resolvability of two closely-spaced signals is an important performance measure for parametric estimation problems. In this paper we investigate the so-called resolution limit (RL) in a MIMO radar context, i.e., the minimum angular separation required to resolve two closely-spaced targets. Due to the limited number of elementary scatterers, the Gaussian modeling of the clutter is inappropriate. In our analysis, we consider a K-distributed clutter which is a well-established approximation of the real clutter. Finally, our RL's expression reveals a number of insightful properties that are discussed in detail and, numerical examples are provided to corroborate the theoretical analysis.

Index Terms— K-distributed clutter, performance analysis, Cramér-Rao bound, resolution limit, MIMO radar.

1. INTRODUCTION

Multiple-input multiple-output (MIMO) radar, by employing multiple, spatially distributed transmitters and receivers to achieve waveform diversity [1–3], has the advantage to fundamentally improve the performance of communication systems. In the past decade, immense academic interest has been created concerning the investigation of new algorithms for target localization in MIMO systems and its performance analysis, in terms of lower bounds for parameter estimation accuracy and resolvability [1, 2, 4–7]. The resolvability problem of two closely-spaced signals is one of the most significant performance measures in estimation theory. In regard to this subject, a number of recent works, e.g., [6–8] have applied the concept of the resolution limit (RL) [9–11] in the MIMO context. In all of these works, however, the radar clutter is exclusively modeled as Gaussian processes, an assumption which can be, unfortunately, unrealistic in real life application. This is due to the fact that, the Gaussian modeling of the clutter, notwithstanding its popularity, loses immediately its validity, when the assumption required for the central limit theorem, i.e., that the received clutter results from a *large number* of independent and identically distributed (i.i.d.) elementary scatterers, does not hold. This is for example the case in the context of low-grazing-angle and/or high-resolution radar [12–14]. For MIMO radar, which generally has a considerably higher resolvability than its traditional phased-array counterpart, Gaussian modeling of the clutter is often considered inadequate due to the limited number of i.i.d. elementary scatterers present in each cell.

To grapple with these non-Gaussian clutter cases, numerous clutter models have been devised, out of which the K-distributed clutter [12, 15, 16] has become a popular one, due to its ability to characterize nonhomogeneous ground clutter as well as spiky sea clutters, as supported by experimental data measurements [12, 16, 17]. The K-distributed clutter is the product of two components: the square root of a gamma process (called the texture) accounting for the local scattering, and a complex Gaussian process (called the speckle) describing the local power changing. A K-distributed clutter is thus fully characterizable by its texture parameters (i.e., the shape and scale parameter of the gamma distribution) and its speckle covariance matrix. Abounding works already exist to investigate detection/estimation algorithms under the K-distributed clutter [12, 15, 16], however, to the resolvability problem of radar targets under the K-distributed clutter, despite all its theoretical significance, no available work in the current literature has yet been dedicated. It is our aim to fill this gap, by addressing the following task: "*What is, in a MIMO radar context under the K-distributed clutter, the minimum angular separation required, under which two targets can still be correctly resolved?*"

The aforementioned concept of the RL serves as the keystone in approaching such a task. The RL is commonly defined as the minimum distance w.r.t. the parameter of interest that allows distinguishing between two closely-spaced sources [9–11] and can be described, respectively, on the basis of three distinctive theories: the mean null spectrum analysis theory [18], the detection theory [10, 19, 20], and finally, the estimation theory, which exploits the definition of the Cramér-Rao bound (CRB) [9, 21, 22]. One prevalent criterion based on the estimation theory, proposed by Smith [9], states that two targets *are resolvable if the distance between the targets (w.r.t. the parameter of interest) is greater than the standard deviation of the distance estimation*. Smith's criterion considers the coupling between the parameters and thus is preferable to other estimation theory based criteria, e.g., the ones of [21, 23]. Furthermore, the RL obtained in Smith's sense has been proved to be closely related to the detection theory based RL [11]. Finally, Smith's criterion enjoys generality as, unlike the mean null spectrum analysis approach, it is not designed for certain specific high-resolution algorithms. In view of these merits, in this paper we focus on Smith's criterion, to evaluate the RL between two closely-spaced targets in a MIMO radar system under the K-distributed clutter, to inspect its various properties, and to reveal emphatically how the choices of the texture parameters can exert a decisive influence on the behavior of the RL.

2. OBSERVATION MODEL

Consider a colocated MIMO radar system with uniform linear arrays (ULAs) both at the transmitter and the receiver, illuminating two far-field, narrowband, point targets [1]. The radar output, without matched filtering, for the lth radar pulse in a coherent processing interval (CPI) is given as the following vector form [7]:

$$\boldsymbol{y}_l(t) = \sum_{i=1}^{2} \alpha_i v_l(f_i) \boldsymbol{a}_{\mathcal{R}}(\omega_i) \boldsymbol{a}_{\mathcal{T}}^T(\omega_i) \boldsymbol{s}_l(t) + \boldsymbol{n}_l(t), \quad t = 1, \ldots, T \text{ and } l = 0, \ldots, L-1, \tag{1}$$

where α_i denotes a complex coefficient proportional to the radar cross section (RCS); $v_l(f_i) = e^{2j\pi f_i l}$ in which f_i represents the normalized Doppler frequency of the *i*th target; T and L denote the number of snapshots per pulse and the number of pulses per CPI, respectively; the transmitting and receiving steering vectors are defined as $\boldsymbol{a}_{\mathcal{T}}(\omega_i) = \left[1, e^{j\omega_i d_{\mathcal{T}}}, \ldots, e^{j\omega_i (M-1) d_{\mathcal{T}}}\right]^T$ and $\boldsymbol{a}_{\mathcal{R}}(\omega_i) = \left[1, e^{j\omega_i d_{\mathcal{R}}}, \ldots, e^{j\omega_i (N-1) d_{\mathcal{R}}}\right]^T$, in which M and N represent the number of sensors at the transmitter and the receiver, respectively; $d_{\mathcal{T}}$ and $d_{\mathcal{R}}$ denote the inter-element spacing for the transmitter and the receiver, respectively; $\omega_i = 2\pi/\lambda \cdot \sin(\theta_i)$ denotes the electrical angle of the *i*th target, in which λ is the wave length and θ_i represents the direction-of-arrival(DOA)/direction-of-departure(DOD) of the *i*th target[1]; $\boldsymbol{s}_l(t)$ and $\boldsymbol{n}_l(t)$ denote the target source vectors and the received clutter vectors for the *l*th pulse, respectively; and $(\cdot)^T$ is the transpose of a matrix.

For no other reason than mathematical succinctness, assume in the remaining part of this paper that there is one radar pulse per CPI, i.e., $L = 1$, which allows us to remove the subscript in the variables $\boldsymbol{y}_l(t)$, $\boldsymbol{s}_l(t)$, $\boldsymbol{n}_l(t)$ and $v_l(f_i)$ and thus transforms Eq. (1) into[2]:

$$\boldsymbol{y}(t) = \sum_{i=1}^{2} \alpha_i \boldsymbol{a}_{\mathcal{R}}(\omega_i) \boldsymbol{a}_{\mathcal{T}}^T(\omega_i) \boldsymbol{s}(t) + \boldsymbol{n}(t), \quad t = 1, \ldots, T. \tag{2}$$

Furthermore, for the convenience of later derivation we define $\Delta = \omega_2 - \omega_1$ representing the angular spacing between the two targets[3]. Therefore the observation model in Eq. (2) can be reformulated as:

$$\boldsymbol{y}(t) = \boldsymbol{V}(t) + \boldsymbol{n}(t), \quad t = 1, \ldots, T; \tag{3}$$

in which $\boldsymbol{V}(t) = \alpha_1 \boldsymbol{a}_{\mathcal{R}}(\omega_1) \boldsymbol{a}_{\mathcal{T}}^T(\omega_1) \boldsymbol{s}(t) + \alpha_2 \boldsymbol{a}_{\mathcal{R}}(\omega_1 + \Delta) \cdot \boldsymbol{a}_{\mathcal{T}}^T(\omega_1 + \Delta) \boldsymbol{s}(t)$. In addition, we make the following assumptions:

A1 The signal source vectors $\boldsymbol{s}(t) = [s_1(t) \ldots s_M(t)]^T$, $t = 1, \ldots, T$ are deterministic.

A2 The received clutter vectors $\boldsymbol{n}(t)$, $t = 1, \ldots, T$ are independent and identically K-distributed vectors represented as the product of two components [24]:

$$\boldsymbol{n}(t) = \sqrt{\tau(t)} \boldsymbol{x}(t), \quad t = 1, \ldots, T. \tag{4}$$

$\tau(t)$, $t = 1, \ldots, T$ (texture terms) are i.i.d. positive random variables following the *gamma distribution*, i.e., $\tau(t) \sim \text{Gamma}(\phi, \varsigma)$, with the shape parameter ϕ and the scale parameter ς, and its conditional pdf is given by:

$$p_\tau(\tau(t); \phi, \varsigma) = \frac{1}{\Gamma(\phi) \varsigma^\phi} \tau(t)^{\phi - 1} e^{-\frac{\tau(t)}{\varsigma}}, \tag{5}$$

where $\Gamma(\phi) = \int_0^{+\infty} x^{\phi-1} e^{-x} \mathrm{d}x$ is the Gamma function. $\boldsymbol{x}(t)$, $t = 1, \ldots, T$ (speckle terms) are i.i.d. N-dimensional circular complex Gaussian vectors with zero mean and second-order moments, uncorrelated with $\tau(t)$:

$$\mathrm{E}\left\{\boldsymbol{x}(i) \boldsymbol{x}^H(j)\right\} = \check{\delta}_{ij} \boldsymbol{\Sigma}, \quad \mathrm{E}\left\{\boldsymbol{x}(i) \boldsymbol{x}^T(j)\right\} = \boldsymbol{0}_{N \times N}, \quad i, j = 1, \ldots, T, \tag{6}$$

in which $\boldsymbol{\Sigma}$ denotes the speckle covariance matrix, $\mathrm{E}\{\cdot\}$ is the expectation operator, $(\cdot)^H$ denotes the conjugate transpose of a matrix, $\check{\delta}_{ij}$ is the Kronecker delta, and $\boldsymbol{0}_{N \times N}$ denotes the $N \times N$ zero matrix.

A3 The unknown parameter vector of our problem is given by[4]:

$$\boldsymbol{\xi} = \left[\Delta, \quad \overline{\alpha}_1, \quad \widetilde{\alpha}_1, \quad \overline{\alpha}_2, \quad \widetilde{\alpha}_2, \quad \phi, \quad \varsigma, \quad \boldsymbol{\zeta}^T\right]^T, \tag{7}$$

where $\overline{(\cdot)}$ and $\widetilde{(\cdot)}$ represent the real and the imaginary part, respectively; $\boldsymbol{\zeta}$ is a vector containing the independent real-valued parameters of the Hermitian matrix $\boldsymbol{\Sigma}$. Consider the angular separation Δ to be our parameter of interest.

Let $\boldsymbol{\chi} = \left[\boldsymbol{y}^T(1), ..., \boldsymbol{y}^T(T)\right]^T$ denote the full observation vector. Since the clutter vectors of different snapshots are i.i.d., the joint pdf of the complete observation data set can be formulated as:

$$p_{\boldsymbol{\chi}}(\boldsymbol{\chi}; \boldsymbol{\xi}) = \prod_{t=1}^{T} \frac{1}{|\pi \boldsymbol{\Sigma}|} q_N\left(\|\gamma(t)\|^2, \phi, \varsigma\right); \tag{8}$$

where

$$q_N\left(\|\gamma(t)\|^2, \phi, \varsigma\right) = \int_0^{+\infty} \tau^{-N}(t) e^{-\frac{\|\gamma(t)\|^2}{\tau(t)}} p_\tau(\tau(t); \phi, \varsigma) \mathrm{d}\tau(t); \tag{9}$$

and $\gamma(t) = \boldsymbol{\Sigma}^{-1/2}(\boldsymbol{y}(t) - \boldsymbol{V}(t))$, representing the spatially whitened noise vector at time t. Accordingly, the log-likelihood function, denoted Λ, can be represented as:

$$\Lambda = \ln p_{\boldsymbol{\chi}}(\boldsymbol{\chi}; \boldsymbol{\xi}) = -T \ln |\pi \boldsymbol{\Sigma}| + \sum_{t=1}^{T} \ln q_N\left(\|\gamma(t)\|^2, \phi, \varsigma\right). \tag{10}$$

3. CRAMÉR-RAO BOUND AND RESOLUTION LIMIT DERIVATION

In order to evaluate the RL in Smith's sense, we have to first obtain the CRB w.r.t. the parameter Δ. The latter, denoted as $\mathrm{CRB}(\Delta)$, is related to the Fisher Information Matrix (FIM) corresponding to $\boldsymbol{\xi}$, denoted by $\boldsymbol{F}$, as $\mathrm{CRB}(\Delta) = \mathrm{CRB}\left([\boldsymbol{\xi}]_1\right) = \left[\boldsymbol{F}^{-1}\right]_{1,1}$.

3.1. Score Functions

The computation of the entries of $\boldsymbol{F}$ involves partial derivatives of the log-likelihood function Λ w.r.t. all elements of $\boldsymbol{\xi}$ (also known as the score functions) and is given as:

$$[\boldsymbol{F}]_{i,j} = \mathrm{E}\left\{\frac{\partial \Lambda}{\partial [\boldsymbol{\xi}]_i} \frac{\partial \Lambda}{\partial [\boldsymbol{\xi}]_j}\right\}. \tag{11}$$

[1] Note that in a colocated MIMO radar context, the DOA and DOD of a target is the same, meaning a target has the same electrical angle at the transmitter and the receiver.

[2] Note that the terms $v(f_i)$, $i = 1, 2$ are always equal to one under the assumption $L = 1$, which therefore will be omitted in the expressions in the remaining part of the paper.

[3] Assume, without loss of generality, that $\omega_2 > \omega_1$, hence $\Delta > 0$.

[4] Here we consider ω_1 to be known while ω_2 unknown (thus Δ unknown), an assumption that makes good sense in many scenarios, e.g., in those where ω_1 represents a cooperative target with known position and ω_2 is the unknown position of a non-cooperative target. We remark, that the extension of this work to the case where both ω_1 and ω_2 are unknown is straightforward.

Introduce the parameter sets $\beta \in \{\Delta, \overline{\alpha}_1, \widetilde{\alpha}_1, \overline{\alpha}_2, \widetilde{\alpha}_2\}$ and $\varpi \in \{\phi, \varsigma\}$. The partial derivatives $\partial\Lambda/\partial[\boldsymbol{\xi}]_i$ are straightforwardly computed as:

$$\frac{\partial\Lambda}{\partial\beta} = -\sum_{t=1}^{T}\mu_{\|\gamma(t)\|^2}\cdot\left(\gamma^H(t)\boldsymbol{\Sigma}^{-\frac{1}{2}}\frac{\partial\boldsymbol{V}(t)}{\partial\beta}+\frac{\partial\boldsymbol{V}^H(t)}{\partial\beta}\boldsymbol{\Sigma}^{-\frac{1}{2}}\gamma(t)\right),$$
$$\beta\in\{\Delta,\overline{\alpha}_1,\widetilde{\alpha}_1,\overline{\alpha}_2,\widetilde{\alpha}_2\}; \tag{12a}$$

$$\frac{\partial\Lambda}{\partial[\boldsymbol{\zeta}]_i} = -\sum_{t=1}^{T}\mu_{\|\gamma(t)\|^2}\cdot\left(\gamma^H(t)\boldsymbol{\Sigma}^{-\frac{1}{2}}\frac{\partial\boldsymbol{\Sigma}}{\partial[\boldsymbol{\zeta}]_i}\boldsymbol{\Sigma}^{-\frac{1}{2}}\gamma(t)\right)$$
$$-T\mathrm{tr}\left\{\boldsymbol{\Sigma}^{-1}\frac{\partial\boldsymbol{\Sigma}}{\partial[\boldsymbol{\zeta}]_i}\right\},\quad i=1,...,N^2; \tag{12b}$$

$$\frac{\partial\Lambda}{\partial\varpi} = \sum_{t=1}^{T}\mu_{\varpi},\quad \varpi\in\{\phi,\varsigma\}; \tag{12c}$$

where tr$\{\cdot\}$ denotes the trace of a matrix, and:

$$\mu_{\|\gamma(t)\|^2} = \left(\frac{\partial q_N(\|\gamma(t)\|^2,\phi,\varsigma)}{\partial\|\gamma(t)\|^2}\right)/q_N(\|\gamma(t)\|^2,\phi,\varsigma)$$
$$= -\frac{\int_0^{+\infty}\tau^{-N-1}(t)e^{-\frac{\|\gamma(t)\|^2}{\tau(t)}}p_\tau(\tau(t);\phi,\varsigma)\mathrm{d}\tau(t)}{\int_0^{+\infty}\tau^{-N}(t)e^{-\frac{\|\gamma(t)\|^2}{\tau(t)}}p_\tau(\tau(t);\phi,\varsigma)\mathrm{d}\tau(t)}; \tag{13a}$$

$$\mu_{\varpi} = \left(\frac{\partial q_N(\|\gamma(t)\|^2,\phi,\varsigma)}{\partial\varpi}\right)/q_N(\|\gamma(t)\|^2,\phi,\varsigma)$$
$$= \frac{\int_0^{+\infty}\tau^{-N}(t)e^{-\frac{\|\gamma(t)\|^2}{\tau(t)}}\frac{\partial p_\tau(\tau(t);\phi,\varsigma)}{\partial\varpi}\mathrm{d}\tau(t)}{\int_0^{+\infty}\tau^{-N}(t)e^{-\frac{\|\gamma(t)\|^2}{\tau(t)}}p_\tau(\tau(t);\phi,\varsigma)\mathrm{d}\tau(t)},\ \varpi\in\{\phi,\varsigma\} \tag{13b}$$

3.2. Entries of $\boldsymbol{F}$

The entries of $\boldsymbol{F}$ are obtained by substituting Eq. (12a)-(12b) into Eq. (11). We use the same methodology as in [25, 26] to obtain the analytical expressions of the FIM's entries, and find that $\boldsymbol{F}$ has the following block-diagonal structure:

$$\boldsymbol{F} = \begin{bmatrix}\boldsymbol{\Phi} & \boldsymbol{0}_{5\times(N^2+2)}\\ \boldsymbol{0}_{(N^2+2)\times5} & \boldsymbol{\Xi}\end{bmatrix}, \tag{14}$$

where

$$\boldsymbol{\Phi} = \begin{bmatrix} f_{\Delta\Delta} & f_{\Delta\overline{\alpha}_1} & f_{\Delta\widetilde{\alpha}_1} & f_{\Delta\overline{\alpha}_2} & f_{\Delta\widetilde{\alpha}_2}\\ f_{\Delta\overline{\alpha}_1} & f_{\overline{\alpha}_1\overline{\alpha}_1} & f_{\overline{\alpha}_1\widetilde{\alpha}_1} & f_{\overline{\alpha}_1\overline{\alpha}_2} & f_{\overline{\alpha}_1\widetilde{\alpha}_2}\\ f_{\Delta\widetilde{\alpha}_1} & f_{\overline{\alpha}_1\widetilde{\alpha}_1} & f_{\widetilde{\alpha}_1\widetilde{\alpha}_1} & f_{\widetilde{\alpha}_1\overline{\alpha}_2} & f_{\widetilde{\alpha}_1\widetilde{\alpha}_2}\\ f_{\Delta\overline{\alpha}_2} & f_{\overline{\alpha}_1\overline{\alpha}_2} & f_{\widetilde{\alpha}_1\overline{\alpha}_2} & f_{\overline{\alpha}_2\overline{\alpha}_2} & f_{\overline{\alpha}_2\widetilde{\alpha}_2}\\ f_{\Delta\widetilde{\alpha}_2} & f_{\overline{\alpha}_1\widetilde{\alpha}_2} & f_{\widetilde{\alpha}_1\widetilde{\alpha}_2} & f_{\overline{\alpha}_2\widetilde{\alpha}_2} & f_{\widetilde{\alpha}_2\widetilde{\alpha}_2}\end{bmatrix}, \tag{15}$$

is a 5×5 symmetric submatrix of $\boldsymbol{F}$ containing FIM entries w.r.t. the target parameters (Δ, $\overline{\alpha}_i$ and $\widetilde{\alpha}_i$, $i=1,2$). The expressions of the entries of $\boldsymbol{\Phi}$ are obtained by invoking Lemma 2 and Lemma 3 proved in [26], and by considering the circularity property that $\mathrm{E}\{\boldsymbol{x}(i)\boldsymbol{x}^T(j)\} = \boldsymbol{0}_{N\times N},\ i,j=1,\ldots,T$ in Eq. (6) and that the speckle is uncorrelated with the texture (hence $\mathrm{E}\{\boldsymbol{\gamma}(t)\boldsymbol{\gamma}^T(t)\}=0$), leading to

$$f_{\beta_1\beta_2} = \frac{2}{N}\mathrm{E}\left\{\sum_{t=1}^{T}\mu^2_{\mu_{\|\gamma(t)\|^2}}\cdot\|\boldsymbol{\gamma}(t)\|^2\cdot\overline{\mathrm{tr}\left\{\frac{\partial\boldsymbol{V}(t)}{\partial\beta_1}\frac{\partial\boldsymbol{V}^H(t)}{\partial\beta_2}\boldsymbol{\Sigma}^{-1}\right\}}\right\}$$
$$=\frac{2\kappa}{N}\sum_{t=1}^{T}\overline{\mathrm{tr}\left\{\boldsymbol{V}_{\beta_1}(t)\boldsymbol{V}^H_{\beta_2}(t)\boldsymbol{\Sigma}^{-1}\right\}},$$
$$\beta_i\in\{\Delta,\overline{\alpha}_1,\widetilde{\alpha}_1,\overline{\alpha}_2,\widetilde{\alpha}_2\},\quad i=1,2; \tag{16}$$

where

$$\kappa = \mathrm{E}\left\{\|\gamma(t)\|^2\cdot\mu^2_{\|\gamma(t)\|^2}\right\}; \tag{17}$$

and

$$\boldsymbol{V}_\Delta(t) = \frac{\partial\boldsymbol{V}(t)}{\partial\Delta} = j\alpha_2\Big(\dot{\boldsymbol{a}}_{\mathcal{R}}(\omega_1+\Delta)\boldsymbol{a}^T_{\mathcal{T}}(\omega_1+\Delta)$$
$$+\boldsymbol{a}_{\mathcal{R}}(\omega_1+\Delta)\dot{\boldsymbol{a}}^T_{\mathcal{T}}(\omega_1+\Delta)\Big)\boldsymbol{s}(t), \tag{18a}$$

$$\boldsymbol{V}_{\overline{\alpha}_1}(t) = \frac{\partial\boldsymbol{V}(t)}{\partial\overline{\alpha}_1} = \boldsymbol{a}_{\mathcal{R}}(\omega_1)\boldsymbol{a}^T_{\mathcal{T}}(\omega_1)\boldsymbol{s}(t), \tag{18b}$$

$$\boldsymbol{V}_{\widetilde{\alpha}_1}(t) = \frac{\partial\boldsymbol{V}(t)}{\partial\widetilde{\alpha}_1} = j\boldsymbol{a}_{\mathcal{R}}(\omega_1)\boldsymbol{a}^T_{\mathcal{T}}(\omega_1)\boldsymbol{s}(t), \tag{18c}$$

$$\boldsymbol{V}_{\overline{\alpha}_2}(t) = \frac{\partial\boldsymbol{V}(t)}{\partial\overline{\alpha}_2} = \boldsymbol{a}_{\mathcal{R}}(\omega_1+\Delta)\boldsymbol{a}^T_{\mathcal{T}}(\omega_1+\Delta)\boldsymbol{s}(t), \tag{18d}$$

$$\boldsymbol{V}_{\widetilde{\alpha}_2}(t) = \frac{\partial\boldsymbol{V}(t)}{\partial\widetilde{\alpha}_2} = j\boldsymbol{a}_{\mathcal{R}}(\omega_1+\Delta)\boldsymbol{a}^T_{\mathcal{T}}(\omega_1+\Delta)\boldsymbol{s}(t); \tag{18e}$$

in which $\dot{\boldsymbol{a}}_{\mathcal{T}}(\cdot) = \boldsymbol{a}_{\mathcal{T}}(\cdot)\odot\boldsymbol{d}_{\mathcal{T}}$, $\dot{\boldsymbol{a}}_{\mathcal{R}}(\cdot) = \boldsymbol{a}_{\mathcal{R}}(\cdot)\odot\boldsymbol{d}_{\mathcal{R}}$, where $\odot$ denotes the Hadamard product, and $\boldsymbol{d}_{\mathcal{T}} = [0, d_{\mathcal{T}}, \ldots, (M-1)d_{\mathcal{T}}]^T$, $\boldsymbol{d}_{\mathcal{R}} = [0, d_{\mathcal{R}}, \ldots, (N-1)d_{\mathcal{R}}]^T$.

The existence of the zero blocks in Eq. (14) follows from the observation that for fixed $\|\gamma(t)\|$, $\partial\Lambda/\partial\beta$, $\beta\in\{\Delta,\overline{\alpha}_1,\widetilde{\alpha}_1,\overline{\alpha}_2,\widetilde{\alpha}_2\}$ are odd functions of $\gamma(t)$, while $\partial\Lambda/\partial[\boldsymbol{\zeta}]_i$, $\partial\Lambda/\partial\phi$ and $\partial\Lambda/\partial\varsigma$ are even functions of $\gamma(t)$. Thus all the entries $\mathrm{E}\{(\partial\Lambda/\partial\beta)(\partial\Lambda/\partial\varepsilon)\}$, $\beta\in\{\Delta,\overline{\alpha}_1,\widetilde{\alpha}_1,\overline{\alpha}_2,\widetilde{\alpha}_2\},\varepsilon\in\{[\boldsymbol{\zeta}]_i,\phi,\varsigma\}$ are even functions of $\gamma(t)$ and thus are equal to zero. This decouples $\boldsymbol{\Phi}$ from $\boldsymbol{\Xi}$, which represents the FIM block w.r.t. the clutter parameters (ϕ, ς and $[\boldsymbol{\zeta}]_i$). As a result, CRB(Δ) can be obtained by the simple inversion of $\boldsymbol{\Phi}$, i.e., CRB$(\Delta) = [\boldsymbol{F}^{-1}]_{1,1} = [\boldsymbol{\Phi}^{-1}]_{1,1}$. Thus the concrete expressions of the entries of $\boldsymbol{\Xi}$ are beyond our concern.

3.3. Smith Equation

Now, in consonance with Smith's criterion [9], these two targets can be angularly resolved if Δ is *greater* than the standard deviation of the estimate of Δ; while the later, under mild conditions [27], can be approximated by $\sqrt{\mathrm{CRB}(\Delta)}$. Thus, the RL of the two targets in our model, henceforth denoted by δ, is equal to the (approximated) standard deviation of its estimate, i.e., δ fulfills the following expression (also known as the *Smith equation*):

$$\delta^2 = \mathrm{CRB}(\delta). \tag{19}$$

It is noticeable from Eq. (18a), (18d) and (18e) that the entries of $\boldsymbol{\Phi}$ are highly non-linear w.r.t. Δ, meaning that all attempts of finding an analytical solution of Eq. (19) are generally difficult without resort to certain means of approximation (e.g., the Taylor expansion), i.e., without impairing the accuracy of the value of δ. This fact, combined with the mathematical difficulty of inverting the 5×5 matrix $\boldsymbol{\Phi}$, makes such an attempt, if still feasible, undesirable. Therefore we shall numerically evaluate the value of δ, to avoid the aforementioned drawbacks and to retain the true, unapproximated value of δ. The results of our evaluation, with all their significance and implications, will be presented in Section 4.

3.4. Calculation of κ

A crucial but tricky point in evaluating the value of δ is the calculation of κ in Eq. (17), as the latter is devoid of any closed-form expression, thus can only be gauged by numerical means. By applying (C.48) and (C.49) in [26]:

$$\kappa = \frac{\int_0^{+\infty} \mu^2_{\|\gamma(t)\|^2} \cdot q_N\left(\|\gamma(t)\|^2, \phi, \varsigma\right) \cdot \|\gamma(t)\|^{2N+1} \, \mathrm{d}\,\|\gamma(t)\|}{\int_0^{+\infty} q_N\left(\|\gamma(t)\|^2, \phi, \varsigma\right) \cdot \|\gamma(t)\|^{2N-1} \, \mathrm{d}\,\|\gamma(t)\|} \tag{20}$$

Substituting Eq. (9) and (13a) into Eq. (20) and then using the generalized Gauss-Laguerre quadrature [28] for all layers of integrations, we obtain:

$$\kappa = \frac{\sum_{m_1=1}^{M_1^{(2N+1)}} \frac{\left(\sum_{m_2=1}^{M_2^{(\phi-1)}} \exp\left(-\frac{x^2_{m_1}}{x_{m_2}\varsigma}\right) \frac{1}{\varsigma} x_{m_2}^{-(N+1)} w_{m_2}\right)^2}{\sum_{m_3=1}^{M_3^{(\phi-1)}} \exp\left(-\frac{x^2_{m_1}}{x_{m_3}\varsigma}\right) x_{m_3}^{-N} w_{m_3}} e^{x_{m_1}} w_{m_1}}{\sum_{m_4=1}^{M_4^{(2N-1)}} \left(\sum_{m_5=1}^{M_5^{(\phi-1)}} \exp\left(-\frac{x^2_{m_4}}{x_{m_5}\varsigma}\right) x_{m_5}^{-N} w_{m_5}\right) e^{x_{m_4}} w_{m_4}}. \tag{21}$$

where x_{m_i}, $i = 1, \ldots, 5$ and w_{m_i}, $i = 1, \ldots, 5$ represent the abscissae and the weights of the generalized Gauss-Laguerre quadrature, respectively; $M_1^{(2N+1)}$, $M_2^{(\phi-1)}$, etc. denote the quadrature orders; with the subscript of each representing the respective parameter of the corresponding abscissa and weight (e.g., $M_1^{(2N+1)}$ means that x_{m_1} and w_{m_1} have $2N+1$ as their parameter). In our simulations, the values of these quadrature orders are empirically chosen as $M_1^{(2N+1)} = 212$, $M_2^{(\phi\pm1)} = 214$, $M_3^{(\phi\pm1)} = 196$, $M_4^{(2N-1)} = 200$, and $M_5^{(\phi\pm1)} = 168$, to generate the most accurate results.

4. NUMERICAL SIMULATIONS

Consider a MIMO radar with $M = 6$ sensors at the transmitter and $N = 8$ at the receiver, both with half-wave length inter-element spacing; the snapshot number per CPI $T = 500$; the complex coefficients $\alpha_1 = 1+j$ and $\alpha_2 = 1-j$; all the real and imaginary parts of the target source vectors $\boldsymbol{s}(t)$'s entries are randomly generated within $[-1, 1]$; while the entries of the speckle covariance matrix $\boldsymbol{\Sigma}$ are generated by: $[\boldsymbol{\Sigma}]_{m,n} = \sigma^2 \cdot 0.9^{|m-n|} e^{j\frac{\pi}{2}(m-n)}$, $m, n = 1, \ldots, N$, where σ^2 denotes the speckle power factor [29].

Note that the texture and speckle are mutually uncorrelated, and that for the K-distributed clutter, the mean of the texture $\mathrm{E}\{\tau(t)\} = \phi\varsigma$, the target-to-clutter ratio (TCR) can be formulated as:

$$\mathrm{TCR} = \frac{\sum_{t=1}^{T} \|\boldsymbol{s}(t)\|^2}{T \cdot \mathrm{E}\left\{\boldsymbol{n}^H(t)\boldsymbol{n}(t)\right\}} = \frac{\sum_{t=1}^{T} \|\boldsymbol{s}(t)\|^2}{T \cdot \phi\varsigma \cdot \mathrm{tr}\left\{\boldsymbol{\Sigma}\right\}}. \tag{22}$$

- We first investigate the respective impact of the texture parameters ϕ and ς on δ, by fixing only one texture parameter and changing the other. In Fig. 1, we plot δ vs. TCR with fixed ς and various ϕ and find that δ increases notably with ϕ. This is because the rise of the shape parameter ϕ makes the clutter more heavy-tailed, thus a larger portion of the clutter power decentralized, leading to a deteriorated δ.
- In Fig. 2 we do the converse, by plotting δ vs. TCR with different ς and fixed ϕ. Fig. 2 shows, quite interestingly, that δ remains substantially the same for, thus could be regarded as independent of, the different choices of ς.
- In Fig. 1 & Fig. 2, where we vary only one texture parameter and fix the other, we have thereby also changed the texture power (and thus also the speckle power, for each specific TCR). In Fig. 3, we fix the texture power $\mathrm{E}\{\tau(t)\} = \phi\varsigma = 4$ and choose several pairs of ϕ and ς corresponding to this power and examine δ in this context. We also plot δ under Gaussian clutter for comparison (for which $\tau(t) = \hat{\delta}(\tau(t)-1)$ with $\hat{\delta}(\cdot)$ denoting the Dirac delta function, leading to $\kappa = N$). Fig. 3 shows that δ rises with a pair of increasing ϕ and decreasing ς; at the same time, δ cannot rise infinitely, and is upper-bounded by δ under Gaussian clutter.

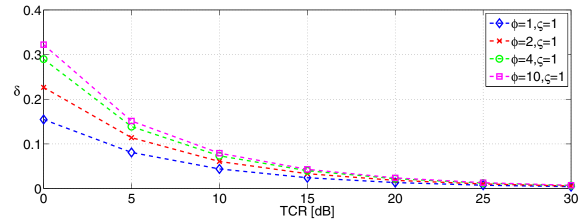

Fig. 1: δ vs. TCR for K-distributed clutter with various ϕ and fixed $\varsigma = 1$.

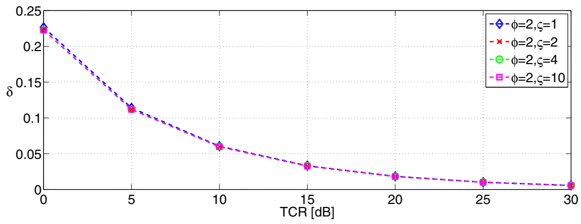

Fig. 2: δ vs. TCR for K-distributed clutter various ς and fixed $\phi = 2$.

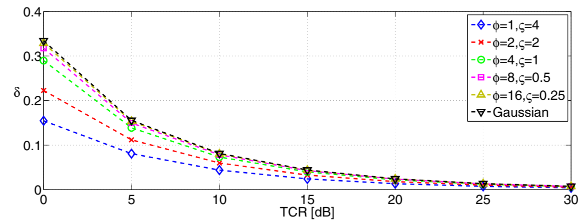

Fig. 3: δ vs. TCR for K-distributed clutter with fixed texture power $\mathrm{E}\{\tau(t)\} = \phi\varsigma = 4$.

5. SUMMARY

We have in this paper investigated the resolvability problem in a MIMO context under the K-distributed clutter, by applying the concept of the RL in Smith's sense. We have firstly derived the FIM expressions, and then by virtue of the Smith equation we have numerically obtained the value of the RL δ. Our simulation concentrates on the impact of texture parameters on δ, and reveals that δ increases with ϕ but remains unreactive to the change of ς. Finally, our results show that δ under all K-distributed clutters, regardless of their texture parameters, is smaller than δ under the Gaussian clutter.

References

[1] J. Li and P. Stoica, *MIMO radar Signal Processing*, Wiley-Interscience, New York, Oct. 2008.

[2] C.-Y. Chen and P. P. Vaidyanathan, "MIMO radar space-time adaptive processing using prolate spheroidal wave functions," *IEEE Trans. Signal Processing*, vol. 56, no. 2, pp. 623–635, Feb. 2008.

[3] I. Bekkerman and J. Tabrikian, "Target detection and localization using MIMO radars and sonars," *IEEE Trans. Signal Processing*, vol. 54, pp. 3873–3883, Oct. 2006.

[4] J. Li and P. Stoica, "MIMO radar with colocated antennas," *IEEE Signal Processing Magazin*, vol. 24, no. 5, pp. 106–114, Sept. 2007.

[5] M. Jin, G. Liao, and J. Li, "Joint DOD and DOA estimation for bistatic MIMO radar," *Elsevier Signal Processing*, vol. 2, pp. 244–251, Feb. 2009.

[6] R. Boyer, "Performance bounds and angular resolution limit for the moving co-located MIMO radar," *IEEE Trans. Signal Processing*, vol. 59, no. 4, pp. 1539–1552, Apr. 2011.

[7] M. N. El Korso, F. Pascal, and M. Pesavento, "On the resolvability of closely spaced targets using a colocated MIMO radar," in *Proc. 46th Asilomar Conference on Signals, Systems and Computers*, Pacific Grove, Nov. 2012, Invited paper.

[8] F. Foroozan, A. Asif, and R. Boyer, "Time reversal MIMO radar: Improved CRB and angular resolution limit," in *Proc. 38th International Conference on Acoustics, Speech, and Signal Processing (ICASSP 2013)*, Vancouver, Canada, May 2013, pp. 4125–4129.

[9] S. T. Smith, "Statistical resolution limits and the complexified Cramér Rao bound," *IEEE Trans. Signal Processing*, vol. 53, pp. 1597–1609, May 2005.

[10] M. Shahram and P. Milanfar, "On the resolvability of sinusoids with nearby frequencies in the presence of noise," *IEEE Trans. Signal Processing*, vol. 53, no. 7, pp. 2579–2588, July 2005.

[11] M. N. El Korso, R. Boyer, A. Renaux, and S. Marcos, "Statistical resolution limit for multiple parameters of interest and for multiple signals," in *Proc. ICASSP*, Dallas, TX, Mar. 2010, pp. 3602–3605.

[12] F. Aluffi Pentin, A. Farina, and F. Zirill, "Radar detection of targets located in a coherent K distributed clutter background," *Radar and Signal Processing, IEE Proceedings F*, vol. 139, no. 3, pp. 239–245, June 1992.

[13] J. B. Billingsley, "Ground clutter measurements for surface-sited radar," Tech. Rep. 780, Massachusetts Inst. Technol., Cambridge, MA, Feb. 1993.

[14] F. Gini, M. V. Greco, M. Diani, and L. Verrazzani, "Performance analysis of two adaptive radar detectors against non-gaussian real sea clutter data," *IEEE Trans. Aerosp. Electron. Syst.*, vol. 36, pp. 1429–1439, Oct. 2000.

[15] E. Conte, M. Longoand, M. Lops, and S. L. Ullo, "Radar detection of signals with unknown parameters in K-distributed clutter," *Radar and Signal Processing, IEE Proceedings F*, vol. 138, no. 2, pp. 131–138, Apr. 1991.

[16] S. Watts, "Radar detection prediction in sea clutter using the compound K-distribution model," *Proc. Inst. Electr. Eng. F*, vol. 132, no. 7, pp. 613–620, Dec. 1985.

[17] T. Nohara and S. Haykin, "Canada east coast trials and the K-distribution," *Proc. Inst. Electr. Eng. F*, vol. 138, no. 2, pp. 82–88, Apr. 1991.

[18] H. Cox, "Resolving power and sensitivity to mismatch of optimum array processors," *J. Acoust. Soc.*, vol. 54, no. 3, pp. 771–785, 1973.

[19] M. Shahram and P. Milanfar, "Imaging below the diffraction limit: A statistical analysis," *IEEE Trans. Image Processing*, vol. 13, no. 5, pp. 677–689, May 2004.

[20] Z. Liu and A. Nehorai, "Statistical angular resolution limit for point sources," *IEEE Trans. Signal Processing*, vol. 55, no. 11, pp. 5521–5527, Nov. 2007.

[21] H. B. Lee, "The Cramér-Rao bound on frequency estimates of signals closely spaced in frequency," *IEEE Trans. Signal Processing*, vol. 40, no. 6, pp. 1507–1517, 1992.

[22] M. N. El Korso, R. Boyer, A. Renaux, and S. Marcos, "Statistical resolution limit of the uniform linear cocentered orthogonal loop and dipole array," *IEEE Trans. Signal Processing*, vol. 59, no. 1, pp. 425–431, Jan. 2011.

[23] H. B. Lee, "The Cramér-Rao bound on frequency estimates of signals closely spaced in frequency (unconditional case)," *IEEE Trans. Signal Processing*, vol. 42, no. 6, pp. 1569–1572, 1994.

[24] K. Yao, "Spherically invariant random processes: Theory and applications," in *Communications, Information and Network Security*, V. K. Bhargava *et al.*, Ed., pp. 315–332. 2002.

[25] K. L. Lange, R. J. A. Little, and J. M. G. Taylor, "Robust statistical modeling using the t distribution," *J. Amer. Stat. Assoc.*, vol. 84, no. 408, pp. 881–896, Dec. 1989.

[26] J. Wang, A. Dogandžić, and A. Nehorai, "Maximum likelihood estimation of compound Gaussian clutter and taget parameters," *IEEE Trans. Signal Processing*, vol. 54, no. 10, pp. 3884–3897, Oct. 2006.

[27] E. L. Lehmann, *Theory of Point Estimation*, Wiley, New York, 1983.

[28] R. A. Thisted, *Elements of Statistical Computing: Numerical Computation*, Chapman & Hall, New York, 1988.

[29] M. Viberg, P. Stoica, and B. Ottersten, "Maximum likelihood array processing in spatially correlated noise fields using parameterized signals," *IEEE Trans. Signal Processing*, vol. 45, no. 4, pp. 996–1004, Apr. 1997.